

How Animals Dance (When You’re Not Looking)

XIAOJUAN WANG, University of Washington, USA

ALEKSANDER HOLYNSKI, UC Berkeley, USA

BRIAN CURLESS, University of Washington, USA

IRA KEMELMACHER-SHLIZERMAN, University of Washington, USA

STEVEN M. SEITZ, University of Washington, USA

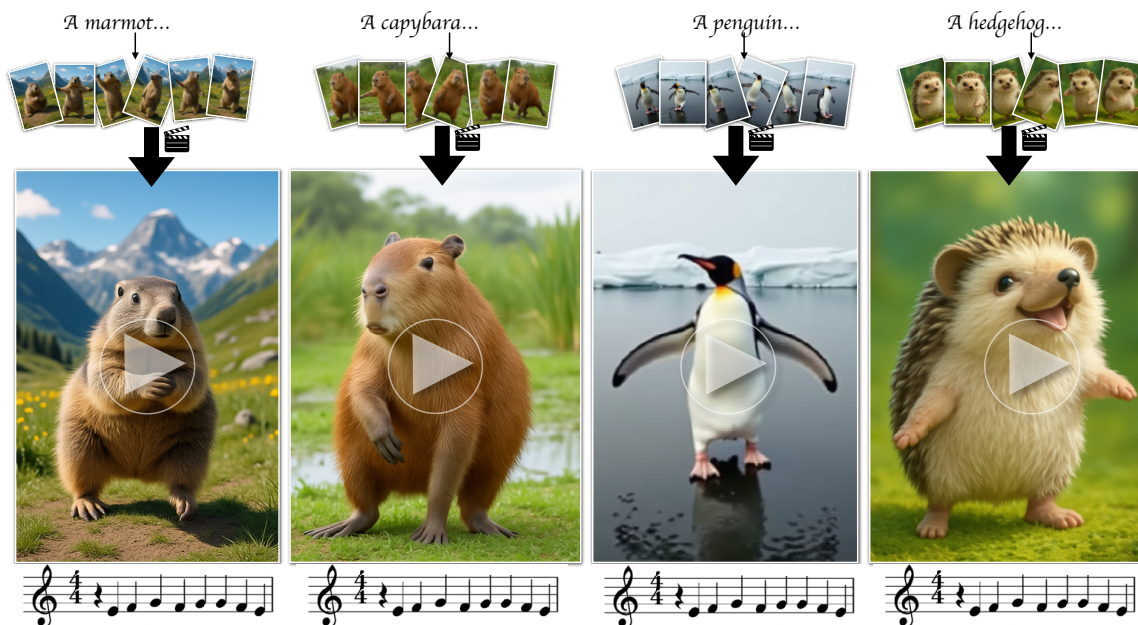


Fig. 1. Starting from a small set of generated keyframes, e.g., a marmot in various poses, our method generates an animal dance video that follows a specified choreography pattern, extracted from a reference dance video.

We present a keyframe-based framework for generating music-synchronized, choreography aware animal dance videos. Starting from a few keyframes representing distinct animal poses—generated via text-to-image prompting or GPT-4o— we formulate dance synthesis as a graph optimization problem: find the optimal keyframe structure that satisfies a specified choreography pattern of beats, which can be automatically estimated from a reference dance video. We also introduce an approach for mirrored pose image generation, essential for capturing symmetry in dance. In-between frames are synthesized using a video diffusion model. With as few as six input keyframes, our method can produce up to 30 second dance videos across a wide range of animals and music tracks. See our project page for more results: how-animals-dance.github.io.

CCS Concepts: • **Computing methodologies** → **Computer vision**.

Additional Key Words and Phrases: dance video generation, diffusion models, vision for graphics

Authors’ addresses: Xiaojuan Wang, xiaojwan@cs.washington.edu, University of Washington, USA; Aleksander Holynski, UC Berkeley, USA, holynski@google.com; Brian Curless, University of Washington, USA, curless@cs.washington.edu; Ira Kemelmacher-Shlizerman, University of Washington, USA, kemelmi@cs.washington.edu; Steven M. Seitz, University of Washington, USA, seitz@cs.washington.edu.

1 INTRODUCTION

Everything in the universe has a rhythm; everything dances.

—Maya Angelou

Humans dance spontaneously to music—just picture a toddler cheerfully bouncing to the beats at a birthday party. Animals can dance too; *Snowball the cockatoo* (Fig. 2)—can perform up to 14 distinct dance movements in response to different musical cues [Keehn et al. 2019]. In fact, our animal friends are probably dancing all the time when we’re not looking. In this paper, we capture this hidden world of animal dance, and expose it *for the first time* to the human population (Fig. 1).

While we happen to be particularly obsessed with dancing animals, this paper introduces a new framework for generating music-synchronized, highly structured, 30 second+ long dance videos. Such capabilities are challenging for current state of the art generative models, most of which are limited to short clips of a few seconds, do not produced synchronized audio and video, and lack intuitive controls for long range motion. Beyond text prompting, most controls for video generation are fine-grained and operate on a single frame at a time, e.g., body pose, camera pose, motion brushes, etc.



Fig. 2. *Snowball the cockatoo*: a real bird that can dance.

In contrast, we introduce *choreography patterns* as a new control for video generation. Specifically, we allow the user to specify a structured sequence of dance moves, or “beats”, e.g., A-B-A-B-C-D-A, where each letter corresponds to a particular move, and constrain the motion in the video to follow that choreography. Furthermore, we show how these choreography patterns can be automatically estimated from existing (human) dance videos.

A well-formed dance follows basic choreographic rules [Chen et al. 2021], which structure the movements to align with the rhythmic flow of the accompanying music, and often involve recurring patterns such as mirroring and repetition to help reinforce the musical structure [Kim et al. 2006, 2003]. We leverage this inherent structure of dance to make the generation task more tractable. As input, we use a collection of initially generated keyframes, each representing a distinct pose. We then formulate the dance synthesis as a graph optimization problem, *i.e.*, find the optimized walk path through the keyframes to satisfy a specified choreography pattern of beats. Each selected keyframe in the path is aligned to a musical beat. The final dance video is produced by synthesizing in-between frames between the keyframes using a generative video inbetweening model [Wang et al. 2024a,b] (Fig. 3).

Beyond 1) introducing a new type of generative video control (choreography patterns), and 2) a practical system for generating music-synchronized dance videos, this paper makes the following technical contributions. First, we introduce a technique for inferring choreography patterns from human dance videos, such as those found on Youtube and TikTok. Second, we formulate the satisfaction of these constraints as a graph optimization problem and solve it. Finally, we demonstrate an approach for pose-mirroring in the image domain, while retaining asymmetries in foreground and background features.

We demonstrate the effectiveness of our method by generating dance videos up to 30 seconds long across approximately 25 animal instances across 10 classes—including marmots, sea otters, hedgehogs, and cats—paired with various songs. These videos represent the first-ever recorded demonstrations of these animals performing such complex musical dance routines and will be studied by generations of zoologists.

2 PRIOR WORK

Music-driven generative dance synthesis. Earlier learning-based approaches developed neural networks that synthesize human dance

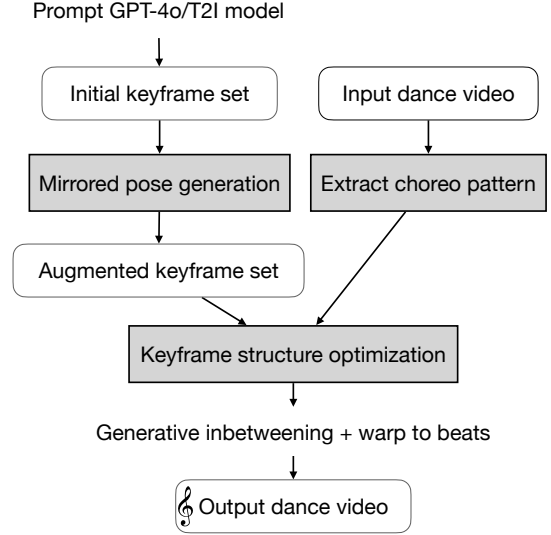


Fig. 3. *System overview*. Given a few initially generated keyframes as input, we generate mirrored counterparts, extract choreography pattern from a dance video, and optimize the keyframe structure accordingly. The final dance is synthesized by generating in-between frames with a video diffusion model and warped to the musical beats. Our method is highlighted in gray.

motion directly from music input [Huang et al. 2020; Lee et al. 2019, 2018; Li et al. 2021; Sun et al. 2020; Zhang et al. 2022]. Recent advances have shifted toward diffusion-based methods [Le et al. 2023; Qi et al. 2023; Tseng et al. 2023], which also focus primarily on generating skeletal motions from music. More recently, some works have begun exploring direct dance video generation using video diffusion models [Ruan et al. 2023; Sun et al. 2020]. However, directly enforcing choreography structure within these frameworks remains challenging. In addition, these learning-based approaches typically require training data—an issue in our case, as dance videos featuring animals are extremely scarce.

Graph-based human motion synthesis. In contrast to learning-based approaches, graph-based frameworks [Chen et al. 2021; Kim et al. 2006, 2003; Manfrè et al. 2016; Ofli et al. 2008] synthesize new motions from an existing dance motion segments database, and cast the dance synthesis as a graph optimization problem: finding an optimal path in the constructed motion graph that aligns with the input music. For example, Kim et al. [Kim et al. 2003] introduced rhythmic and beat-based constraints to guide the path search, while more recent work *ChoreoMaster* [Chen et al. 2021] incorporated richer choreography rules, requiring not only structural alignment with music but also stylistic compatibility.

Our approach follows this paradigm but differs in key ways. First, instead of relying on a motion capture database, we take a small set of keyframes of an animal or subject as input. We augment this set by generating mirrored pose images, creating a complete keyframe set for dance synthesis. The graph is constructed over these keyframes, and a video diffusion model is applied to generate realistic in-between frames along the optimized walk path, producing the final dance video. Second, while basic choreography rules can be inferred from the musical structure as done in [Chen et al.

2021], different performers may interpret the same piece differently. As such, we propose a way to extract choreography patterns directly from a reference dance video and use it as the control.

Anthropomorphic character animation. Given a reference image, character image animation, generates videos following a target human skeletal pose sequence. While existing methods [Hu 2024; Hu et al. 2025] are primarily designed for human figures, recent work [Tan et al. 2024] extends to anthropomorphic characters by learning generalized motion representation. However, it remains favor human-like anatomy, generating animals with features like elongated limbs. They also struggle to generate high-fidelity videos from a single image when handling long and diverse sequences, such as a 30-second dance. In contrast, our method does not rely on per-frame human skeleton pose as guidance. Instead, we use a small set of keyframes generated from text prompt as a pose alternative, and synthesize intermediate frames using a generative inbetweening model. Since our approach is keyframe-based and choreographically structured, it is not constrained by video length and can scale to longer dance sequences.

3 APPROACH

We begin by generating a small set of keyframes $\{I_k\}_{k=0}^{K-1}$, each depicting the subject, e.g., a marmot, in different poses while maintaining a consistent background and static camera view (see Section 4.1 for details). Our goal is to synthesize a dance video of the input animal from the provided keyframes, synchronized to the beats and following the choreography pattern extracted from a reference dance video.

We first introduce how we extract the choreography pattern directly from a human dance video in Section 3.1. Since motion mirroring is an essential component of dance, we then present our approach for generating a mirrored pose counterpart for each keyframe to augment the keyframe set in Section 3.2. Finally, in Section 3.3, we present how to synthesize the full dance video using the complete set of keyframes, including mirrored ones, to follow the choreography pattern.

3.1 Choreography Pattern Labeling

Choreography are closely tied to the rhythmic structure of music. In music theory, a *beat* is the basic temporal unit, while a *bar* (or measure) groups a fixed number of beats. The *meter* defines how beats are grouped and emphasized within the bar, and is indicated by a time signature, e.g., 2/4, 3/4, 4/4, where the upper number specifies beats per bar, and the lower number denotes the note value that receives one beat. In this work, we focus on music with a 4/4 time signature—each bar contains four quarter note beats—the most common structure in popular music.

Problem definition. Given a 4/4 music track with a synchronized dance video, we begin by detecting the beat times $\mathcal{B} = \{t_0, t_1, \dots, t_{N-1}\}$, assuming a total of N beats, corresponding to $\frac{N}{4}$ bars. Based on the beat times, we construct a sequence of motion segments $\mathcal{S} = \{s_0, s_1, \dots, s_{\frac{N}{2}-1}\}$ where each segment s_i spans from beat t_{2i} to beat t_{2i+1} . Each bar thus yields two motion segments: one from the first to the second beat, and another from the third to the fourth beat, aligning with the 4/4 music structure where major movements typically

begin on accented beats and end on weak ones, whereas transitions occur across weak-to-accented intervals. The “choreo pattern” labeling task outputs a sequence of labels $\mathcal{L} = \{l_0, l_1, \dots, l_{\frac{N}{2}-1}\}$, e.g., A-A’-B-C-D-D, where each l_i corresponds to motion segment s_i . Distinct motions receive different labels, identical motions share the same one, and mirrored motions are indicated by prime-labeled counterparts (e.g., A and A’).

Motion segments quantization. We formulate motion segment sequence labeling as a quantization problem: clustering similar motion segments and assigning each a cluster ID as its label. Each segment s_i of length T_i is represented by the SMPL-X [Pavlakos et al. 2019] pose sequence recovered from the video: $s_i = \{(\theta_{t_i} \in \mathbb{R}^{3 \times (J+1)}, \tau_{t_i} \in \mathbb{R}^3)\}_{t_i=0}^{T_i}$, where θ_{t_i} contains per-joint axis-angle rotation for $J = 21$ body joints in addition to a joint for global rotation (the 0-th joint), and τ_{t_i} denotes the global translation in 3D space.

For clustering, we focus solely on poses—ignoring global translations—to capture distinctive motion patterns. The distance between two SMPL-X poses is defined as the average geodesic distance across joints:

$$d_\theta(\theta_1, \theta_2) = \frac{1}{J} \sum_{j=0}^J \|\log(R(\theta_1^j)^T R(\theta_2^j))\|_F \quad (1)$$

where $R(\theta^j)$ converts the axis-angle representation of joint j into a rotation matrix. To account for slight temporal offsets between beats, we compute the distance between two motion segments using dynamic time warping (DTW), with d_θ as the local cost metric between poses. The clustering function C is then defined as:

$$C(\mathcal{S}; \text{DTW}_{d_\theta}, \epsilon_\theta) \rightarrow \{C_1, C_2, \dots, C_C\} \quad (2)$$

where $\bigcup_{c=1}^C C_c = \mathcal{S}$, with $C_i \cap C_j = \emptyset$, for $i \neq j$. Segments within the same cluster satisfy: $\text{DTW}_{d_\theta}(s_i, s_j) < \epsilon_\theta$, $\forall s_i, s_j \in C_c$.

Mirrored motion segments detection. After the quantization stage, we identify mirrored motion segments in two steps.

Mirrored pose clusters. A mirrored joint rotation is defined by reflecting the axis-angle vector across the sagittal (YZ) plane: $\mathcal{F}(\theta^j) = (\omega_x, -\omega_y, -\omega_z)$, where $\theta^j = (\omega_x, \omega_y, \omega_z)$. Then a mirrored pose θ' is obtained by applying this reflection to each joint after left-right joint swapping:

$$\theta'^j = \mathcal{F}(\theta^{\pi(j)}) \quad \text{for } j = 0, \dots, J \quad (3)$$

here $\pi(j)$ denotes the left-right joint permutation (e.g. swapping left/right arms, legs, and shoulders), and for central joints (e.g., spine, neck, head), $\pi(j) = j$, so only the reflection is applied.

Two clusters C_a and C_b are considered mirrored if there exists at least one pair of segments $s_i \in C_a, s_j \in C_b$, such that the mirrored version of s_i , denoted by $s'_i = \{\theta'_{t_i}\}_{t_i=0}^{T_i}$, is similar to s_j under dynamic time warping: $\text{DTW}_{d_\theta}(s'_i, s_j) < \epsilon_{\theta'}$. The resulting set of mirrored cluster pairs is: $\mathcal{M} = \{(C_a, C_b) \mid \exists s_i \in C_a, s_j \in C_b, \text{DTW}_{d_\theta}(s'_i, s_j) < \epsilon_{\theta'}\}$.

Mirrored motion directions within a cluster. For clusters without a mirrored counterpart, we further check whether they can be internally partitioned into two directionally mirrored groups. We first extract the overall motion direction \vec{d}_{s_i} of each motion segment

s_i using its global translation: $\vec{d}_{s_i} = (\tau_{t_i}^{T_i} - \tau_{t_i}^0) / \|\tau_{t_i}^{T_i} - \tau_{t_i}^0\|$, where $\tau_{t_i}^0$ and $\tau_{t_i}^{T_i}$ denote the segment’s start and end positions, respectively.

To identify mirrored directions, each motion direction \vec{d}_{s_i} is reflected across the YZ plane as $\vec{d}'_{s_i} = \text{diag}([-1, 1, 1])\vec{d}_{s_i}$. We then perform bipartite matching to find mirror pairs (s_i, s_j) that satisfy $\|\vec{d}'_{s_i} - \vec{d}_{s_j}\| < \epsilon_d$. If valid pairs are found, we assign all matched segments into two directionally consistent groups based on their directional similarity. The original cluster C_i is then partitioned into two mirrored subgroups (C_i^0, C_i^1) , which are then added to the mirrored cluster set \mathcal{M} .

Finally, we assign a unique label to each cluster. For each mirrored pair $(C_a, C_b) \in \mathcal{M}$, we assign a base label l_a (e.g. A) to segments in C_a , and its mirrored label l'_a (e.g. A') to segments in C_b . Clusters without a mirrored counterpart are assigned a distinct label without a prime.

3.2 Mirrored Pose Image Generation

To augment the keyframe set with mirrored counterparts, we generate visually consistent keyframe pairs for each input pose. This process (Fig. 4) involves fine-tuning a text-to-image model with ControlNet, generating mirrored edge maps, and re-generating the original keyframes for consistency. In the end, we get a complete set of consistent keyframes $\mathcal{I} = \{I_0, \dots, I_{K-1}, I'_0, \dots, I'_{K-1}\}$, where I'_k is the mirrored version of I_k .

Fine-tuning. We fine-tune a pretrained text-to-image model on the input keyframes set, overfitting it to capture the appearance of the specific input subject instance and the background. To provide structural guidance, we incorporate ControlNet [Zhang et al. 2023] using the canny edge maps extracted from the input images as a conditional input. We use the prompt format: “A photo of [V] [subject class name] dancing [background description].”, where [V] is a unique token for identifying the subject **instance** rather than **class**. The placeholders [subject class name] and [background description] are replaced with the actual class name of the subject and background description. For example, “A photo of [V] marmot dancing with alpine landscape as background.”

Mirrored edge generation. To generate mirrored pose images, We first extract the subject mask using SAM [Kirillov et al. 2023]. We then construct a unified background canny edge map by inpainting and stitching the background edges from all input keyframes. For each keyframe, we extract the subject’s edge map and horizontally flip it to create a mirrored subject edge map. This flipped edge map is then composited with the shared background edge map to generate a full mirrored edge map, which is used as input to the fine-tuned model to generate the corresponding mirrored image.

Keyframes re-generation. The original keyframes may contain slight inconsistencies in the background due to generation instability. Additionally, the fine-tuned model may introduce subtle color shifts during inference. To ensure visual consistency among the augmented keyframes set, we regenerate the original keyframes using the same model and shared background edge map (see Fig. 5 for an example).

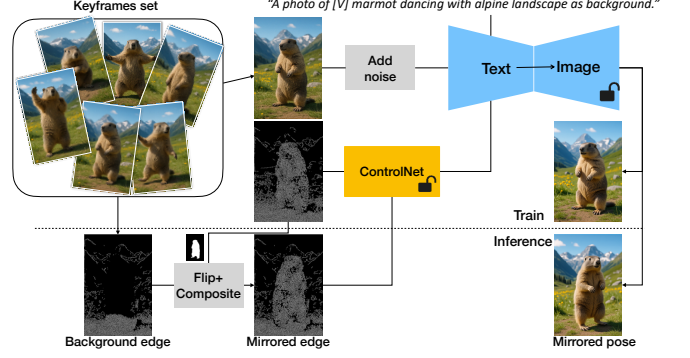


Fig. 4. *Mirrored pose generation.* We fine-tune a text-to-image model with ControlNet using the canny edges extracted from each keyframe as conditioning. During inference, mirrored pose images are generated by flipping only the subject edges and using an inpainted background edge composed from the keyframe set.

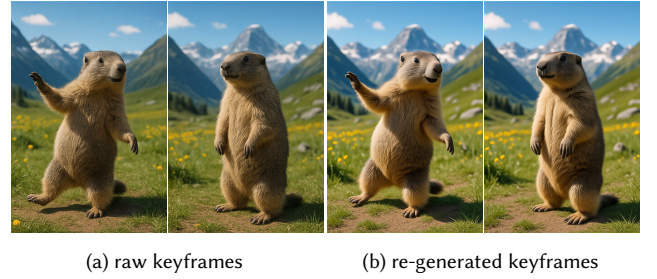


Fig. 5. Improving visual consistency by re-generating keyframes with shared background edges.

Implementation details. We use FLUX.1-dev and Xlabs-AI/flux-controlnet-canny as the pretrained text-to-image and controlnet model. We fine-tune them jointly with a LoRA rank of 16 for 500 epochs, Training on 6 keyframes takes around 90 minutes on a single A100 GPU. Canny edges are extracted using threshold values of (50, 100).

3.3 Choreography Pattern Driven Dance Synthesis

Given the augmented keyframe set $\mathcal{I} = \{I_0, \dots, I_{K-1}, I'_0, \dots, I'_{K-1}\}$, where I'_k denotes the mirrored counterpart of keyframe I_k , and the choreography pattern label sequence $\mathcal{L} = \{l_0, l_1, \dots, l_{\frac{N}{2}-1}\}$, the goal is to find an optimal walk path $\mathcal{P} = \{I_{p_0}, I_{p_1}, \dots, I_{p_{N-1}}\}$ through the keyframe set, and the i -th keyframe I_{p_i} in the path corresponds to the i -th beat. We then apply video diffusion model to generate in-between frames, finally producing the final dance video.

Since each label l_i corresponds to a motion segment between keyframe pairs $(I_{p_{2i}}, I_{p_{2i+1}})$, we cast path planning as a graph optimization, where each node represents a candidate keyframe pair. The choreography label sequence \mathcal{L} specifies assignment constraints: same labels map to the same pair, distinct labels to distinct pairs, and mirrored labels to mirrored pairs. The object is to assign each label l_i to a node such that these constraints are met while minimizing the total transition cost along the path.

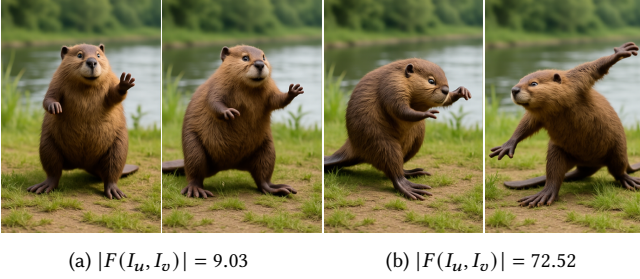


Fig. 6. Keyframe pairs with excessively small or large motion are excluded from the graph nodes.

Keyframe graph construction. We construct the keyframe graph $G = (V, E)$ as a directed graph, where each node $(I_u, I_v) \in V$, with $I_u \neq I_v$, represents an ordered pair of keyframes from the augmented keyframe set \mathcal{I} . Note $(I_u, I_v) \neq (I_v, I_u)$. Each node corresponds to a potential dance segment from I_u to I_v , and each edge $(I_u, I_v) \rightarrow (I_w, I_x) \in E$, with $I_v \neq I_w$, represents a valid transition between segments.

To ensure both expressive motion and synthesis feasibility, we filter nodes based on the average per-pixel flow magnitude $|F(I_u, I_v)|$, computed over the foreground region of the subject. Nodes with flow that is too small (insufficient motion) or too large (challenging for video synthesis) are discarded, as shown in Fig. 6. Only node pairs with acceptable motion range are retained:

$$V = \{(I_u, I_v) \mid M_{\text{low}} < |F(I_u, I_v)| < M_{\text{high}}\} \quad (4)$$

To make the synthesized dance smooth and fluid, we define the edge cost between two nodes as the flow magnitude between the end keyframe of the first node and start one of the next node: $\mathcal{T}((I_u, I_v) \rightarrow (I_w, I_x)) = |F(I_v, I_w)|$. We prune high-cost transitions by including only edges with flow below a threshold:

$$E = \{((I_u, I_v) \rightarrow (I_w, I_x)) \mid |F(I_v, I_w)| < M_{\text{high}}\} \quad (5)$$

We also define a mirroring function $\mu : V \rightarrow V$ over graph node such that two nodes are mirrored if and only their respective keyframes are mirrored: $\mu((I_u, I_v)) = (I'_u, I'_v)$.

Graph optimization. We define a node assignment function: $\phi : \mathcal{L} \rightarrow V$, which maps each choreography label $l_i \in \mathcal{L}$ to a graph node $(I_u, I_v) \in V$, forming a walk path through the keyframe graph. The goal is to find the optimal assignment ϕ^* that minimizes the total transition cost across the sequence:

$$\phi^* = \operatorname{argmin} \sum_{i=0}^{\frac{N}{2}-2} \mathcal{T}(\phi(l_i), \phi(l_{i+1})) \quad (6)$$

subject to the following constraints:

$$l_i \neq l_j \Leftrightarrow \phi(l_i) \neq \phi(l_j) \quad (7)$$

$$l'_i \neq l_j \Leftrightarrow \phi(l_i) = \mu(\phi(l_j)) \quad (8)$$

To ensure visual variety and avoid redundancy, we introduce two additional constraints:

(1) Different labels cannot map to partially mirrored node pairs—defined as nodes sharing one keyframe (in any order), with the other keyframes

mirrored:

$$l_i \neq l_j \Rightarrow (I_a, I_b) \neq (I_c, I_d) \quad (9)$$

where $\phi(l_i) = (I_a, I_b)$, $\phi(l_j) = (I_c, I_d)$.

(2) Consecutive, distinct, and non-mirrored labels must not be assigned to nodes that share a keyframe, to prevent unnecessary single keyframe repetition.

$$l_i \neq l_{i+1}, l'_i \neq l_{i+1} \Rightarrow (I_a \neq I_c \wedge I_b \neq I_d) \quad (10)$$

where $\phi(l_i) = (I_a, I_b)$, $\phi(l_{i+1}) = (I_c, I_d)$.

3.4 Warp to Music

We generate the final dance video by applying a video diffusion model to synthesize in-between frames along the optimized keyframe walk path $\mathcal{P} = \{I_{p_0}, I_{p_1}, \dots, I_{p_{N-1}}\}$, where each keyframe I_{p_i} corresponds to beat position i . Note that since there are motion repetition in the choreography, we only have to synthesize videos between unique keyframe pairs. In practice, we use Framer [Wang et al. 2024a], which generates 14 in-between frames, and we assume a fps of 25. To synchronize with the music, we warp the video timeline such that the timing of every keyframe in \mathcal{P} align with the corresponding beat time in the audio. Following the visual rhythm strategy from [Davis and Agrawala 2018], we accelerate the warping rate into beat points and decelerate before and after to preserve beat saliency while ensuring temporal smoothness.

4 EXPERIMENTS

4.1 Keyframes Generation

We generate initial keyframes set by prompting a text-to-image model, such as FLUX to generate an image grid with consistent keyframes using prompt template like “a 3x2 grid of frames, showing 6 consecutive frames from a video clip of [DESCRIPTION PROMPT]”. For example, the description prompt might be “a marmot dancing wildly in the wild alpine landscape, striking a variety of fun and energetic poses”. The same prompt format can also be used with GPT-4o’s image generation modules, which supports even finer specifications. For instance, one can specify: “Generate a grid with 2 rows and 3 columns. Depict a quokka with distinct poses with a wild background. The postures should feel natural for the quokka’s anatomy....”. In all of our results, we use a total of 6 input keyframes.

4.2 Choreography Pattern Labeling

We collect a total of 20 dance video clips featuring various 4/4 music tracks from Youtube and Tiktok, ranging from 12s to 25s in length. To create ground truth, we manually annotate the choreography pattern label sequence. We then evaluate our method in Section 3.1 by comparing our extracted label sequences against the ground truth ones. Beat times are detected using Librosa, and SMPL-X pose sequences are recovered from the videos using GVHMR [Shen et al. 2024]. We set the threshold values as follows: $\epsilon_\theta = 0.21$, $\epsilon_{\theta'} = 0.25$ and $\epsilon_d = 0.1$. Specifically, we evaluate two aspects: (1) Clustering accuracy, where each unique label—including mirrored variants—is treated as a distinct cluster. We assess the clustering results using standard metrics: Adjusted Rand Index (ARI) and Normalized Mutual Information (NMI); (2) Mirror detection accuracy, where

Clustering		Mirroring		
ARI \uparrow	NMI \uparrow	Precision \uparrow	Recall \uparrow	F1 \uparrow
0.94	0.98	0.93	0.91	0.92

Table 1. Evaluation on choreography pattern labeling.

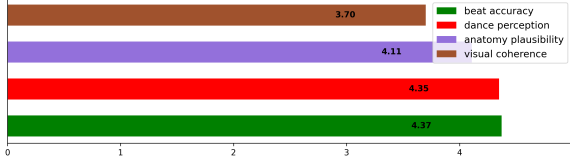


Fig. 7. User study results. Green: Beat accuracy; Red: Dance perception; Purple: Anatomy plausibility; Brown: Visual coherence.

we compute precision and recall based on the correctly identified mirrored motion segments pairs.

We report the results in Table 1. Our training-free extraction method achieves overall strong quantization accuracy, effectively differentiating different motion patterns. For mirroring, our prediction occasionally misses mirrored pairs, typically in cases where the poses are symmetrical but exhibit subtle mirroring in head or body orientation. Since our method also can output representative motions for each choreography label, users can more easily visualize the structure and manually correct annotation errors if needed.

4.3 Dance Results

We generate a collection of input keyframe grids featuring approximately 25 animal instances. The animal classes include *marmot*, *capybara*, *hedgehog*, *meerkat*, *penguin*, *sea otter*, *cat*, *raccoon*, *quokka*, *beaver* and others. We also incorporate anthropomorphic characters such as *Elmo*. For the video results, we generate dance sequences for these instances using six popular song clips, ranging from 16 to 30 seconds in length, with choreography patterns extracted from the corresponding YouTube videos. While we showcase our method using these examples, it can adapt to any choreography patterns paired with music. Selected results are shown in Fig. 9 and Fig. 12, and we highly recommend viewing the supplementary video for the full experience.

User study. Since there are no real animal dance videos or existing methods for direct comparison, we conducted a user study to evaluate our approach. We used 40 generated dance videos across 6 different songs, and invited 31 participants to take part. Each participant was presented a random set of 8 dance videos and asked to rate the following aspects on a scale from 0 to 5: (1) *Beat accuracy*—Does the movement of the animal appear synchronized with the music beat? (2) *Dance perception*—How confident are you that this is a dance rather than random motion? (3) *Anatomical plausibility*—Does the animal’s appearance align with its anatomical structure? (4) *Visual coherence*— Does the video looks visually coherent? The responses are shown in Fig. 7. Our generated dance videos obtained average score of 4.37, 4.35, 4.11, and 3.70 for these factors, respectively.

4.4 Dance Controllability

Given the same choreography pattern for the dance, the user can use pose-grid template to guide the input keyframe poses, control the



Fig. 8. Keyframe pose grid mimicking. Top row: A keyframe pose grid template showing six distinct poses of a capybara. Middle and bottom rows: A meerkat and a hedgehog mimicking the capybara’s poses, while preserving their own anatomical structure and personality, generated using GPT-4o.

allowed motion range in the graph, and define custom constraints during graph optimization.

Pose-grid template control. Given a keyframe pose grid as template, we prompt GPT-4o to generate a new grid in which another animal “mimics” each pose from the original, though the poses are not expected to be exact same since different animals have different anatomical structures. This template may come from a previously generated grid (see Fig. 8 for an example) or be extracted from a human dance video by identifying distinct poses. This provides a way to guide or customize the input poses, which allows to generate dance videos where different animals dance alike (see supplementary video for examples).

Motion range control. The threshold parameters M_{low} and M_{high} control the range of allowed motion magnitudes between keyframes. A typical setting is $M_{\text{low}} \geq 12$. and $M_{\text{high}} \leq 60$. Within this range, lowering M_{low} and increasing M_{high} introduces more candidate nodes and transitions, potentially resulting in richer and more expressive dances.

User custom constraints control. During graph optimization, users can specify hard constraints on node assignments—for instance, enforcing preferred keyframe pair(s) for specific label(s). Additionally, for some dance, mirrored poses happen at the start and end of a choreography label. When such mirrored pose pairs are detected for a specific label, we can enforce corresponding node assignments during optimization. For example, such labels have to be assigned to nodes (I_u, I_v) where $I_v = I'_u$. This allows closer alignment with the reference choreography.

5 FAILURES

In the keyframe graph, we use average per-pixel flow magnitude between two keyframes as a proxy for motion strength. However, this measure becomes unreliable in cases where the two keyframes represent mirrored side views, where the flow magnitude fails to

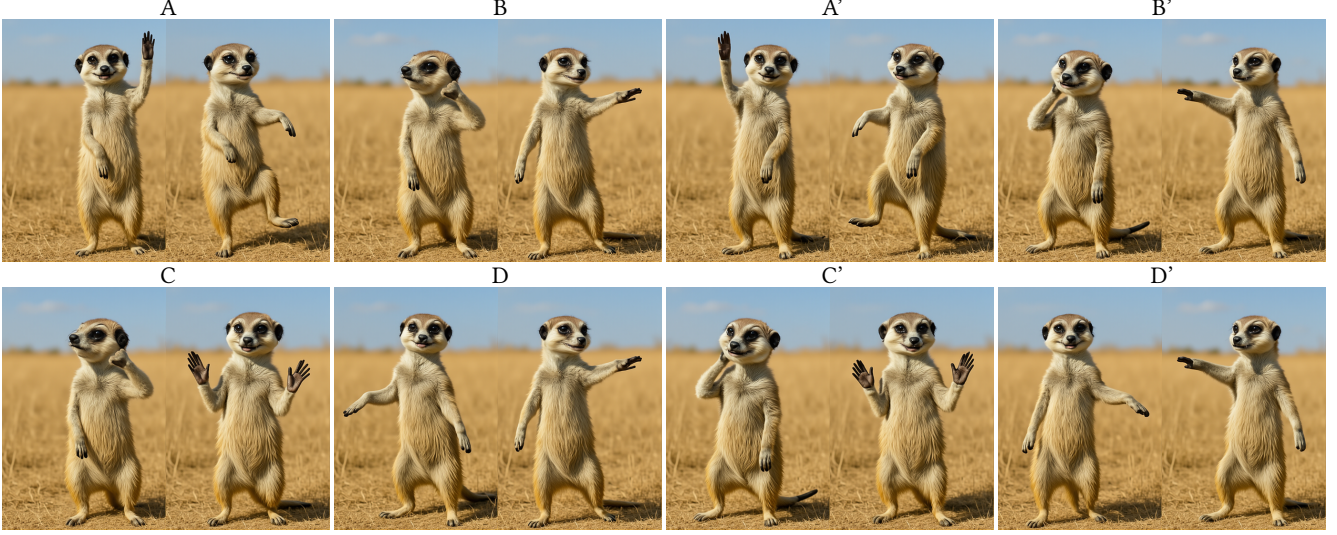


Fig. 9. Selected keyframes from our generated dance video set to the *Bumblebee* song. The choreography pattern follows a reference dance extracted from Youtube video [GIq7ZgmxE2w], from 15.5s to 45.5s: A-B-A'-B'-C-D-C'-D'-A-B-A'-B'-C-D-C'-D'-E-F-G-G-G-G-H-H-H'-H'-G-G-G-G-H-H.

reflect the true motion complexity between poses. For example, in Fig. 10, the average flow magnitude from the left one to the right one is $|F(I_u, I_v)| = 36.81$, which appears moderate due to incorrect correspondences between opposite sides. In reality, this motion is difficult for the video model to synthesize.



Fig. 10. *Failures*. While average flow magnitude from the left one to the right one $|F(I_u, I_v)| = 36.81$ is not large, the motion is hard to synthesize for video model.

6 DISCUSSIONS

6.1 Comparison with Anthropomorphic Animation

Another potential relevant line of work for generating animal dance videos is character animation, which animates an input image using a pose sequence, typically extracted from human motion videos. However, transferring human poses to animals remains an open challenge due to the need to solve complex correspondence problems across different body morphologies and modalities, let alone dealing with long and diverse pose sequences as in dance. As an example, we experimented with generating such videos using Animate-X [Tan et al. 2024]: we extract pose sequences from a real dance video and use GPT-4o to generate an input image of a marmot that mimics the human pose from the first frame, providing a better start point for animation. As shown in Figure 11, the results look blurry and the animated marmot taking on human-like body shapes.

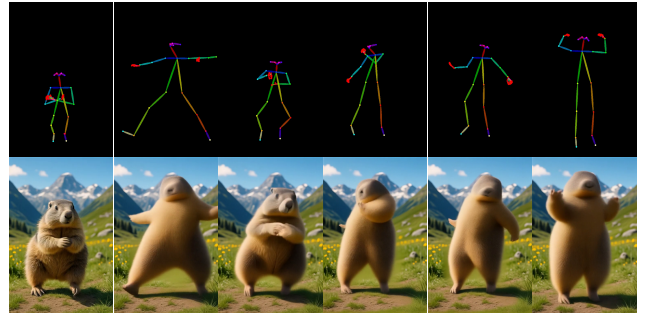


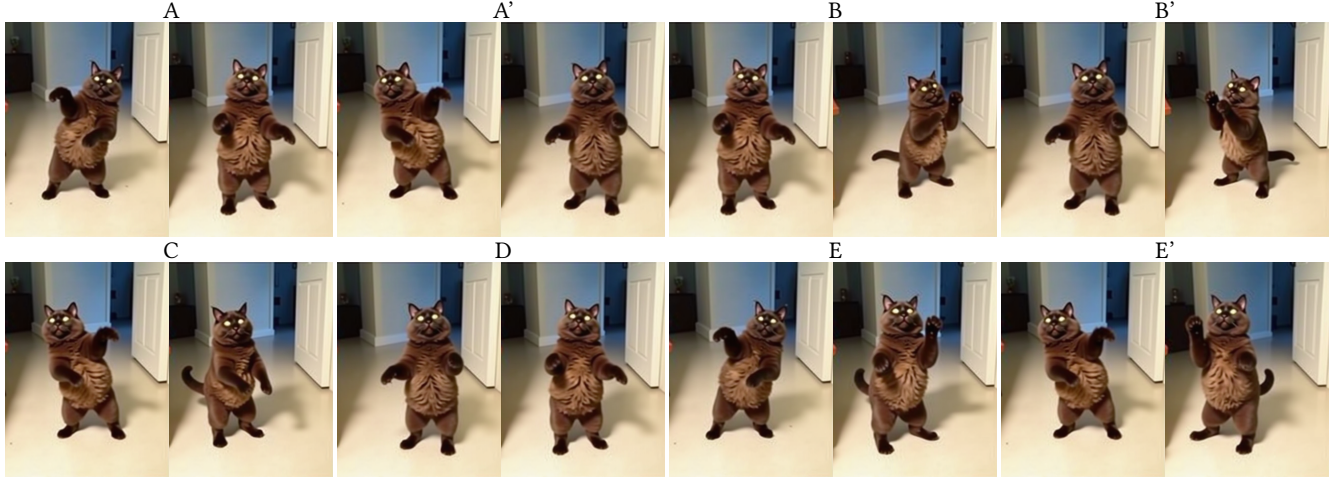
Fig. 11. Example results using character animation method. Top row: pose sequence extracted from real dance video (Youtube shorts, [jkRIIH42Vo8]). Bottom row: animation results from applying the pose sequence to the leftmost image using Animate-X [Tan et al. 2024].

6.2 Limitations

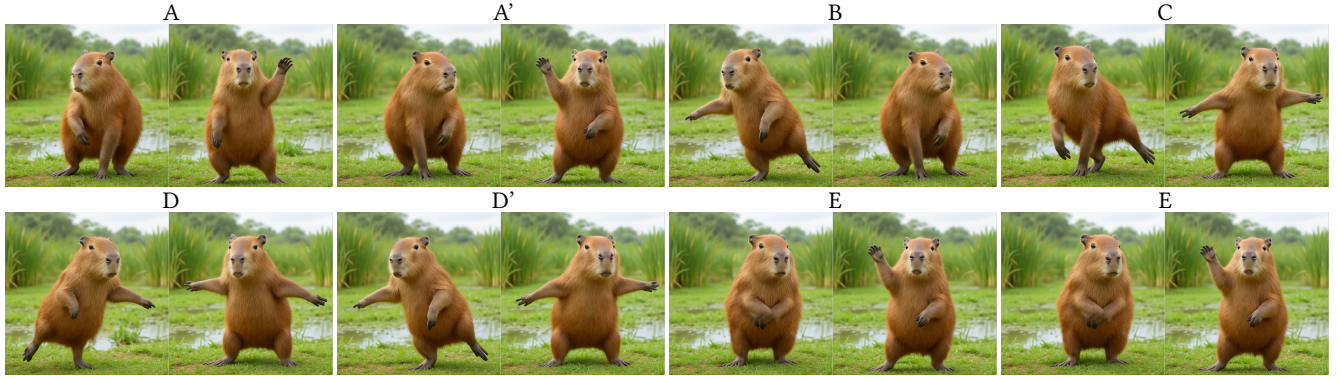
We use an offline video diffusion model to generate short motion segments between keyframes, for example, 0.5s for a 120 BPM song. While the results are often visually coherent, the motion can sometimes appear unrealistic; animals may appear to slide or morph between poses rather than moving in a physically plausible way. This reflects the current limitations of video diffusion models in producing naturalistic motion for articulated subjects. However, with continued advances in large-scale video diffusion models, we are optimistic that these issues can be addressed in the future.

6.3 Future Work

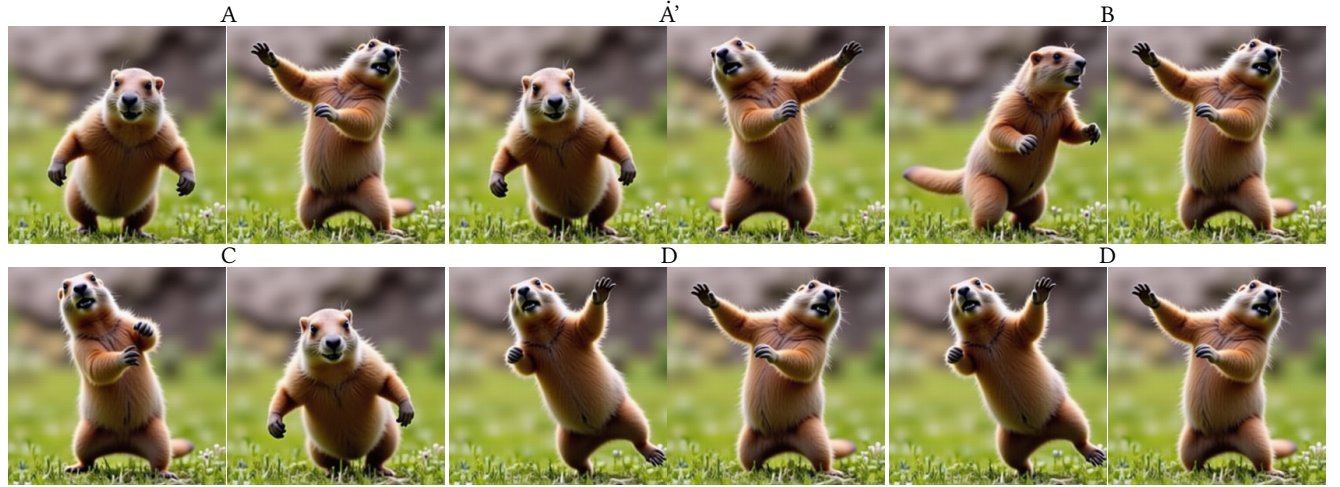
To generate more advanced and musically aligned dances, two directions can be explored: (1) *dance motion realism*: the motions generated by the video diffusion model may not always reflect plausible or expressive dance motion. Incorporating priors that favor



(a) Selected keyframe walk path set to *Uptown Funk* song. Choreography pattern extracted from Youtube video [U9Zj1BaH01c], from 16.0s to 36.0s: A-A'-A-A'-A-A'-B-B'-C-D-E-E'-E-E'.



(b) Selected keyframes from our generated dance video set to the *APT.* song. The choreography pattern follows a reference dance extracted from Youtube video [D]z1zlm73HI], from 11.0s to 37.0s: A-A'-A-A'-A-A'-B-C-A-A'-A-A'-A-A'-B-C-D-D'-D-D'-E-E'-E'-E'-D-D'-D-D'-E-E-E'-E'.



(c) Selected keyframes from our generated dance video set to the *Can't Stop Feeling* song. The choreography pattern follows a reference dance extracted from Youtube video [xyMBnn3dzdU], from 59.0s to 79.0s: A-A'-B-C-D-D-D-D-E-E'-E-E'-F-F'-F-F'-A-A'-B-C-D-D-D-D-E-E'-E-E'-F-F'-F-F'.

Fig. 12. *Dance results.* Keyframe pairs are labeled by the choreography pattern label. The sequence should be read from left to right across the top row, followed by left to right across the bottom row. See supplementary for the full dance video with music.

natural, dance-like movement could improve alignment with musical context. (2) *style compatibility*: although our method follows the choreography pattern, it does not consider musical style. Modeling genre-specific movement characteristics could enhance the stylistic coherence of generated dances.

6.4 Conclusion

We present a novel keyframe-based paradigm for generating music-synchronized, choreography-aware animal dance videos. Our work opens up exciting opportunities for creative and fun applications of dancing animals in entertainment and social media.

Acknowledgments. We thank Tong He and Baback Elmieh for helpful discussions and feedback. This work was supported by the UW Reality Lab and Google.

REFERENCES

- Kang Chen, Zhipeng Tan, Jin Lei, Song-Hai Zhang, Yuan-Chen Guo, Weidong Zhang, and Shi-Min Hu. 2021. Choreomaster: choreography-oriented music-driven dance synthesis. *ACM Transactions on Graphics (TOG)* 40, 4 (2021), 1–13.
- Abe Davis and Maneesh Agrawala. 2018. Visual rhythm and beat. *ACM Transactions on Graphics (TOG)* 37, 4 (2018), 1–11.
- Li Hu. 2024. Animate anyone: Consistent and controllable image-to-video synthesis for character animation. In *Proceedings of the IEEE/CVF Conference on Computer Vision and Pattern Recognition*. 8153–8163.
- Li Hu, Guangyuan Wang, Zhen Shen, Xin Gao, Dechao Meng, Lian Zhuo, Peng Zhang, Bang Zhang, and Liefeng Bo. 2025. Animate Anyone 2: High-Fidelity Character Image Animation with Environment Affordance. *arXiv preprint arXiv:2502.06145* (2025).
- Ruozi Huang, Huang Hu, Wei Wu, Kei Sawada, Mi Zhang, and Daxin Jiang. 2020. Dance revolution: Long-term dance generation with music via curriculum learning. In *International conference on learning representations*.
- R Joanne Jao Keehn, John R Iversen, Irena Schulz, and Aniruddh D Patel. 2019. Spontaneity and diversity of movement to music are not uniquely human. *Current Biology* 29, 13 (2019), R621–R622.
- Jae Woo Kim, Hesham Fouad, and James K Hahn. 2006. Making Them Dance.. In *AAAI Fall Symposium: Aurally Informed Performance*, Vol. 2. 2.
- Tae-hoon Kim, Sang Il Park, and Sung Yong Shin. 2003. Rhythmic-motion synthesis based on motion-beat analysis. *ACM Transactions on Graphics (TOG)* 22, 3 (2003), 392–401.
- Alexander Kirillov, Eric Mintun, Nikhila Ravi, Hanzi Mao, Chloe Rolland, Laura Gustafson, Tete Xiao, Spencer Whitehead, Alexander C. Berg, Wan-Yen Lo, Piotr Dollár, and Ross Girshick. 2023. Segment Anything. *arXiv:2304.02643* (2023).
- Nhat Le, Tuong Do, Khoa Do, Hien Nguyen, Erman Tjiputra, Quang D Tran, and Anh Nguyen. 2023. Controllable group choreography using contrastive diffusion. *ACM Transactions on Graphics (TOG)* 42, 6 (2023), 1–14.
- Hsin-Ying Lee, Xiaodong Yang, Ming-Yu Liu, Ting-Chun Wang, Yu-Ding Lu, Ming-Hsuan Yang, and Jan Kautz. 2019. Dancing to music. *Advances in neural information processing systems* 32 (2019).
- Juheon Lee, Seohyun Kim, and Kyogu Lee. 2018. Listen to dance: Music-driven choreography generation using autoregressive encoder-decoder network. *arXiv preprint arXiv:1811.00818* (2018).
- Ruilong Li, Shan Yang, David A Ross, and Angjoo Kanazawa. 2021. Ai choreographer: Music conditioned 3d dance generation with aist++. In *Proceedings of the IEEE/CVF international conference on computer vision*. 13401–13412.
- Adriano Manfrè, Ignazio Infantino, Filippo Vella, and Salvatore Gaglio. 2016. An automatic system for humanoid dance creation. *Biologically Inspired Cognitive Architectures* 15 (2016), 1–9.
- Ferda Ofli, Yasemin Demir, Yücel Yemez, Engin Erzin, A Murat Tekalp, Koray Balci, İdil Kızıoğlu, Lale Akarun, Cristian Canton-Ferrer, Joëlle Tilmann, et al. 2008. An audio-driven dancing avatar. *Journal on Multimodal User Interfaces* 2 (2008), 93–103.
- Georgios Pavlakos, Vasileios Choutas, Nima Ghorbani, Timo Bolkart, Ahmed A. A. Osman, Dimitrios Tzionas, and Michael J. Black. 2019. Expressive Body Capture: 3D Hands, Face, and Body from a Single Image. In *Proceedings IEEE Conf. on Computer Vision and Pattern Recognition (CVPR)*. 10975–10985.
- Qiaosong Qi, Le Zhuo, Aixi Zhang, Yue Liao, Fei Fang, Si Liu, and Shuicheng Yan. 2023. Diffdance: Cascaded human motion diffusion model for dance generation. In *Proceedings of the 31st ACM International Conference on Multimedia*. 1374–1382.
- Ludan Ruan, Yiyang Ma, Huan Yang, Huiguo He, Bei Liu, Jianlong Fu, Nicholas Jing Yuan, Qin Jin, and Baining Guo. 2023. Mm-diffusion: Learning multi-modal diffusion models for joint audio and video generation. In *Proceedings of the IEEE/CVF Conference on Computer Vision and Pattern Recognition*. 10219–10228.
- Zehong Shen, Huaijin Pi, Yan Xia, Zhi Cen, Sida Peng, Zechen Hu, Hujun Bao, Ruizhen Hu, and Xiaowei Zhou. 2024. World-Grounded Human Motion Recovery via Gravity-View Coordinates. In *SIGGRAPH Asia Conference Proceedings*.
- Guofei Sun, Yongkang Wong, Zhiyong Cheng, Mohan S Kankanhalli, Weidong Geng, and Xiangdong Li. 2020. Deepdance: music-to-dance motion choreography with adversarial learning. *IEEE Transactions on Multimedia* 23 (2020), 497–509.
- Shuai Tan, Biao Gong, Xiang Wang, Shiwei Zhang, Dandan Zheng, Ruobing Zheng, Kecheng Zheng, Jingdong Chen, and Ming Yang. 2024. Animate-x: Universal character image animation with enhanced motion representation. *arXiv preprint arXiv:2410.10306* (2024).
- Jonathan Tseng, Rodrigo Castellon, and Karen Liu. 2023. Edge: Editable dance generation from music. In *Proceedings of the IEEE/CVF Conference on Computer Vision and Pattern Recognition*. 448–458.
- Wen Wang, Qiuyu Wang, Kecheng Zheng, Hao Ouyang, Zhekai Chen, Biao Gong, Hao Chen, Yujun Shen, and Chunhua Shen. 2024a. Framer: Interactive frame interpolation. *arXiv preprint arXiv:2410.18978* (2024).
- Xiaojuan Wang, Boyang Zhou, Brian Curless, Ira Kemelmacher-Shlizerman, Aleksander Holynski, and Steven M Seitz. 2024b. Generative inbetweening: Adapting image-to-video models for keyframe interpolation. *arXiv preprint arXiv:2408.15239* (2024).
- Lymin Zhang, Anyi Rao, and Maneesh Agrawala. 2023. Adding conditional control to text-to-image diffusion models. In *Proceedings of the IEEE/CVF International Conference on Computer Vision*. 3836–3847.
- Mingao Zhang, Changhong Liu, Yong Chen, Zhenchun Lei, and Mingwen Wang. 2022. Music-to-dance generation with multiple conformer. In *Proceedings of the 2022 International Conference on Multimedia Retrieval*. 34–38.